

Direct Power Control of Doubly-Fed Generator Based Wind Turbine Converters to Improve Low Voltage Ride-Through during System Imbalance

Murali M. Baggu
Sr. R&D Engineer
Broadstar Wind Systems
muralimohan@ieee.org

Luke D. Watson
ECE Department
Missouri S&T
ldwxf5@mst.edu

Jonathan W. Kimball
ECE Department
Missouri S&T
kimballjw@mst.edu

Badrul H. Chowdhury
ECE Department
Missouri S&T
bchow@mst.edu

Abstract— A novel control technique using direct active and reactive power control called Direct Power Control (DPC) is discussed for Low Voltage Ride Through (LVRT) of DFIG based wind turbine converters. This controller eliminates the conventional current loops and uses delta modulation comparators, which yields a faster response. The switching of the converter is done using a simple optimum switching table. This control achieves real and reactive power stability with simple active and reactive power control variables. A modified DPC algorithm is proposed to eliminate the current harmonics created by DPC during system disturbances. The practical verification of DPC is carried out by a scaled converter. The control is coded in C and implemented on a TMS320F2812 DSP. The converter using DPC is tested for system unbalance conditions created by an Industrial Power Corruptor (IPC) in the laboratory.

I. INTRODUCTION

The new grid code requirements for wind power integration state that doubly fed induction generator (DFIG) controllers should be capable of overcoming temporary voltage disturbances [1]. They should remain online instead of tripping due to low voltage. This work addresses the design of controllers that would keep the wind turbine in stable operation during an external fault that causes the voltage to drop up to 60% for two seconds. The focus is on the control of the grid-side converter. If the grid-side converter is capable of controlling power flow and maintaining dc bus voltage, then the DFIG will stay online during the disturbance.

A fast acting controller that eliminates the conventional current control and acts directly upon the real and reactive power of the system is proposed by [2]. As this control acts directly according to the error in the real and reactive power flows, this control is called Direct Power Control (DPC). In DPC, the power required for the converter is commanded using the instantaneous voltages and currents whether they are balanced or not. A modified DPC algorithm is derived below

to reduce current harmonics that occur in the grid-side converter during disturbances.

II. DPC OPERATION AND SIMULATION

The single line diagram of a PWM converter is shown in Fig. 1. v_{abc} represents the source or the line voltage and v_{alblcl} represents the voltage of the converter that can be controlled by the DC link. The voltage of the converter depends upon the switching sequence of the converter and the magnitude of the DC voltage. The series inductance of the line and the dc bus capacitance provides boost characteristics for the converter from the AC to the DC side. The flow of current from the source to the load is governed by the difference between the source voltage and the converter voltage. The line inductance provides stiff current characteristics to the source whereas the bus capacitance provides stiff voltage characteristics to the dc link. Typically the source voltage is assumed to be constant, although this is not true in case of system imbalance or during a transient. Hence the flow of the current in the circuit is governed by the magnitude and angle of the converter voltage.

A. DPC Switching States and Delta Modulation

The switching states of a voltage source inverter are based on the space vector modulation approach presented in [3]. The magnitude and angle of the voltage vector can either be increased or decreased by applying appropriate vectors in the α - β plane. In DPC, an optimal switching table based on the analysis in [2],[4] is used for the instantaneous control of real and reactive power. When applying the zero vector, the choice between U_0 (000) or U_7 (111) depends on the converter legs switching during change of states. The three phase instantaneous real and reactive power is estimated by the scalar and vector product of the instantaneous voltages and

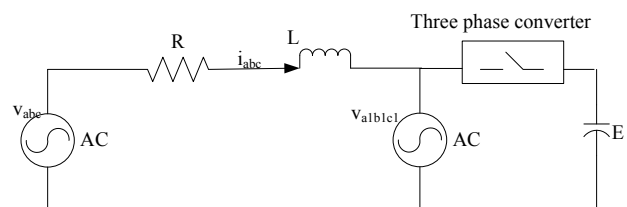


Figure 1. Single line diagram of the PWM converter

This work was supported in part by the U.S. National Science Foundation under Grant ECS-0523897. Mr. Watson is being supported on a Fellowship from the US Dept. of Education.

currents as in (1) and (2), respectively.

$$p = (v_a i_a + v_b i_b + v_c i_c) \quad (1)$$

$$q = \frac{1}{\sqrt{3}} \{ i_a (v_b - v_c) + i_b (v_c - v_a) + i_c (v_a - v_b) \} \quad (2)$$

The commanded real and reactive powers are compared with the estimated power from (1-2). The error is digitized using a delta modulation as follows:

$$\begin{aligned} \text{For reactive power: } d_q &= 1 \text{ for } q < q_{\text{ref}} \quad d_q = 0 \text{ for } q > q_{\text{ref}} \\ \text{For active power: } d_p &= 1 \text{ for } p < p_{\text{ref}} \quad d_p = 0 \text{ for } p > p_{\text{ref}} \end{aligned}$$

The vector position is estimated using the angle of the source voltage in the stationary reference frame, as indicated in (3). The digitized outputs along with the vector position are fed to the optimum switching table. The vector position (θ) is calculated in the range of -180° to 180° and the situation of $V_\alpha = 0$ is eliminated by using the abc to $\alpha\beta$ reference frame block in PLECS[®] block set.

$$\theta = \tan^{-1} \left(\frac{V_\beta}{V_\alpha} \right) \quad (3)$$

A simulation was performed in Matlab/Simulink[®] using PLECS. The block diagram is shown in Fig. 2.

Several simulations have been performed and are shown in Fig. 3. In all cases, a 60% voltage dip occurs in phase A from

0.3 s to 0.8 s. The response of a conventional controller is shown in Fig. 3(a). Figs. 3(b) and 3(c) show the response with DPC. DPC has significantly less power ripple and dc voltage ripple, but also has some distortion in the phase currents.

III. MODIFIED DIRECT POWER CONTROL

In order to decrease the distortion in the currents of the DPC, a hybrid approach similar to that presented in [5] is proposed. In this approach the real and reactive power references for the DPC are appended with powers due to the imbalance. The negative sequence voltages contribute significantly to power imbalance. Neglecting the negative sequence current components, the real and reactive power equations due to the imbalance are modified as in (4) and (5).

$$P_{imb} = v_{dne} i_{dpe} + v_{qne} i_{qpe} \quad (4)$$

$$Q_{imb} = v_{dne} i_{qpe} - v_{qne} i_{dpe} \quad (5)$$

The partial simulation diagram showing the addition of unbalanced power commands is shown in Fig. 4. Notch filters are used for positive and negative sequence separation, and the negative sequence voltages are used to correct for imbalance.

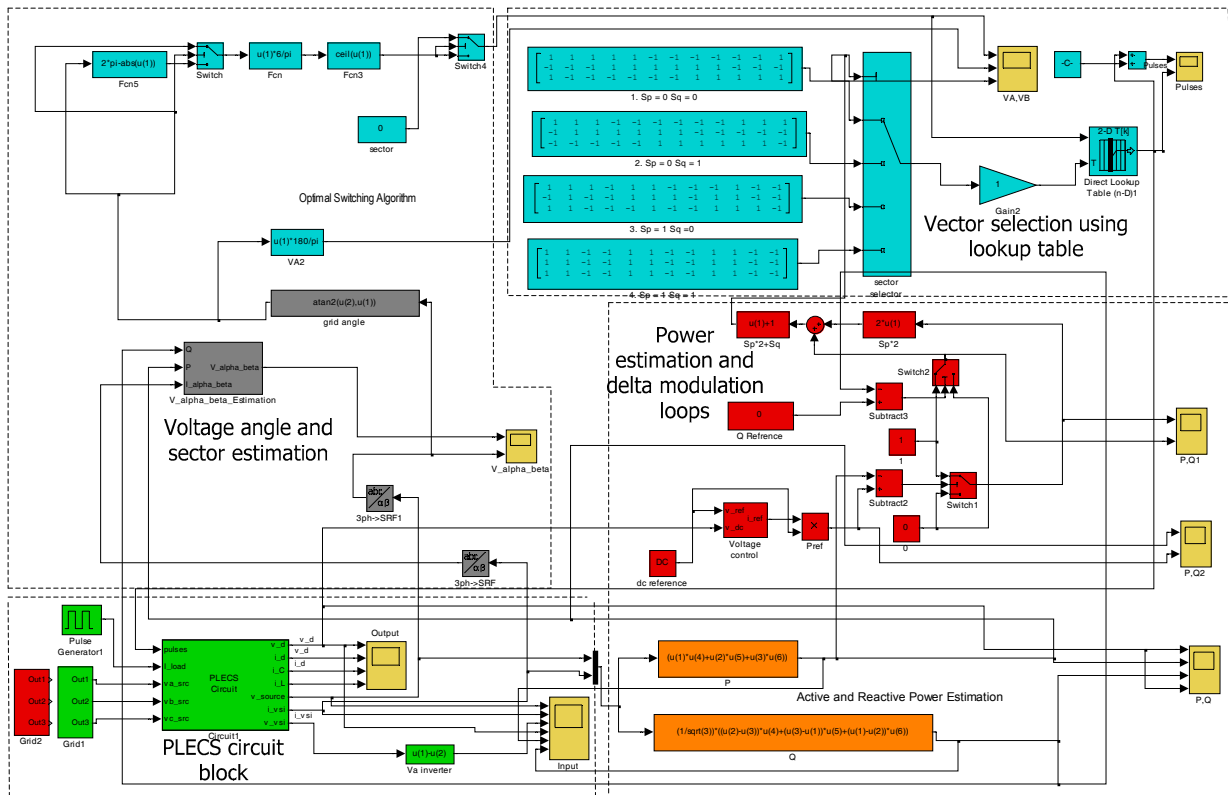
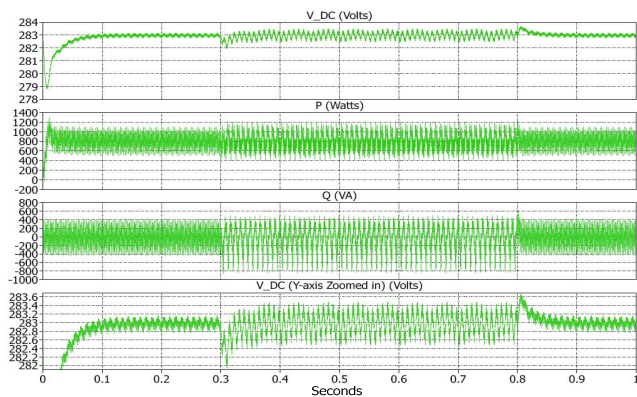
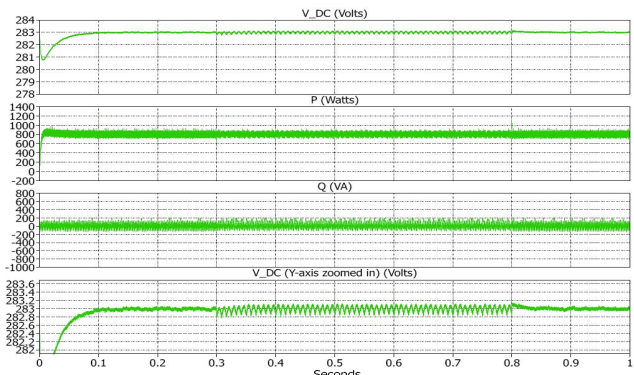


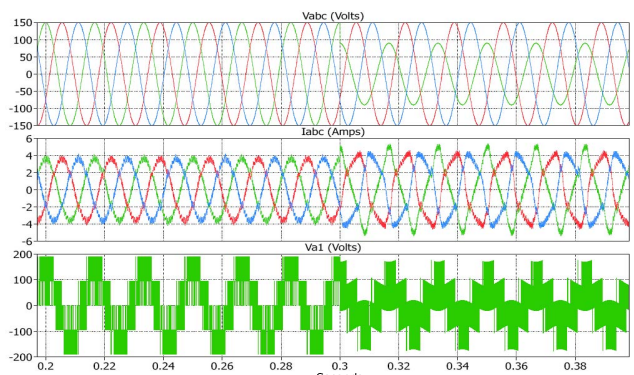
Figure 2. DPC structure for voltage source converter



(a)



(b)



(c)

Figure 3. Grid side converter simulations for a voltage dip of 60%. (a) Conventional current control; (b) and (c) DPC. In (a) and (b), traces are DC bus voltage, real power, reactive power, and zoomed bus voltage. In (c), plots are three-phase source voltage, three-phase line current, and phase A line-to-neutral voltage.

The modified DPC was simulated for the same 60% voltage dip in the input as for the normal DPC. The simulation results are shown in Figure 5. Table 1 shows the comparison of peak-to-peak ripple DC link voltage, real power and reactive powers of the 60% voltage dip. The source currents are less distorted than the normal DPC due to added unbalance in real and reactive power compensation. The trade-off is that the DC link voltage, real power and reactive power have slightly higher oscillations than the normal DPC but have lesser oscillations than the conventional current control

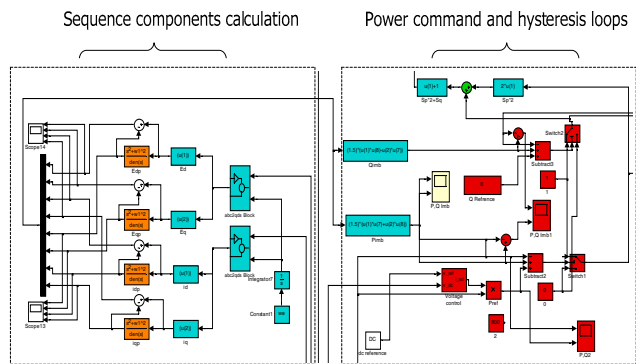
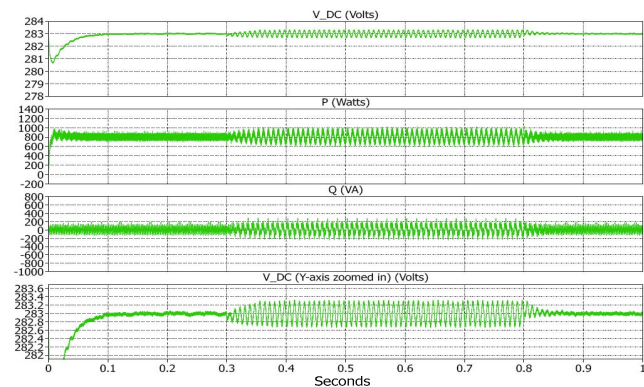


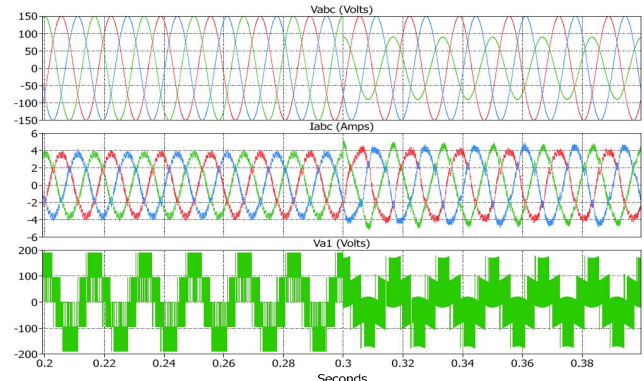
Figure 4. Partial block diagram of MPDC

TABLE I. COMPARISON OF RIPPLE WHEN USING DIFFERENT CONTROL METHODS.

Control Min/Max	DC Link Voltage (283V)	Real Power (800 Watts)	Reactive Power (0VA)
Conventional	282.4/283.4	500/1100	-800/400
DPC	282.8/283.1	730/870	-100/100
MDPC	282.4/283.2	600/1000	-200/200



(a)



(b)

Figure 5. Grid side converter simulation results using MPDC. From top: (a) DC bus voltage, real power, reactive power, and zoomed bus voltage; (b) three-phase source voltage, three-phase line currents, and phase A switched output voltage.

technique. Imbalance power compensation retains the same settling time and overshoot as that of the normal DPC as there is no addition of new controllers. Four new notch filters are added to the circuit which adds computational complexity. A compromise between current distortion and power oscillations needs to be considered when choosing a normal DPC or a modified DPC.

IV. PRACTICAL IMPLEMENTATION

A diagram of the practical implementation is shown in Figure 6. Due to limitations associated with the protection circuitry, the 230 V 3-phase source is connected to a 3-phase variable transformer to step the voltage down. The output of the variable transformer is connected to a delta-wye transformer, which connects to the Industrial Power Corrupter (IPC). The IPC is capable of creating voltage sags to imitate actual conditions on the grid during a disturbance. The delta-wye transformer ensures that the uncorrupted voltage source is balanced.

V_a , V_b , V_c , I_a , I_b , I_c , and V_{DC} are retrieved by the Sensor Board and converted to 0-3V by the Analog Board. A TMS320LF2812 DSP samples the signals and calculates the appropriate vector to apply at a rate of 20 kHz. A sixpack IGBT module, International Rectifier CPV364MU, is used for switching.

The control was implemented using the TMS320LF2812 DSP. The experimental results in Figure 7 demonstrate that the coded algorithm is capable of maintaining the dc link voltage. The currents are more distorted in the experimental results and the powers have greater oscillations, but the real and reactive powers are controlled by the DPC. Fig. 7 shows the experimental results under no fault.

A voltage sag of 30% on V_a is applied to the system for

three cycles as shown in Figure 8. In this case the DC link voltage does not vary during the fault and stays flat. Hence the DPC is capable of riding through these post fault recovery sags and operates normally for voltages greater than 30%.

V. CONCLUSIONS

The controllers based on DPC and MDPC are fast acting; hence they are suitable for sudden grid and wind disturbances. Direct power control is capable of low voltage ride-through (LVRT) for wind turbines and can replace conventional current control. MDPC retains the advantages of DPC and improves current waveform fidelity.

ACKNOWLEDGMENT

This work was funded by the U.S National Science Foundation (NSF) under grant ECS-0523897 and the Electrical and Computer Engineering Department at Missouri University of Science and Technology, Rolla. Mr. Watson is being supported on a fellowship from the US Department of Education.

REFERENCES

- [1] R. Zavadil, N. Miller, A. Ellis, E. Muljadi, E. Camm, and B. Kirby, "Queuing Up: Interconnecting Wind Generation into the Power System," *IEEE Power and Energy Magazine*, vol. 5 pp. 47-58, November/December 2005.
- [2] T. Noguchi, H. Tomiki, S. Kondo, I. Takahashi, "Direct power control of PWM converter without power-source voltage sensors," *IEEE Trans. Ind. Appl.*, vol. 34, pp. 473-479, May/June 1998.
- [3] H. W. Van der Broeck, H-C Skudelny and G V Stanke, "Analysis and realization of a pulsewidth modulator based on voltage space vectors," *IEEE Trans. Ind. Appl.*, vol 24, pp. 142-150, January/February 1988.
- [4] M. Malinowski, M. P. Kazmierkowski, S. Hansen et, al "Virtual-Flux-based Direct power Control of Three-Phase PWM Rectifiers," *IEEE Trans. Ind. Appl.*, . vol. 37, July/August 2001.

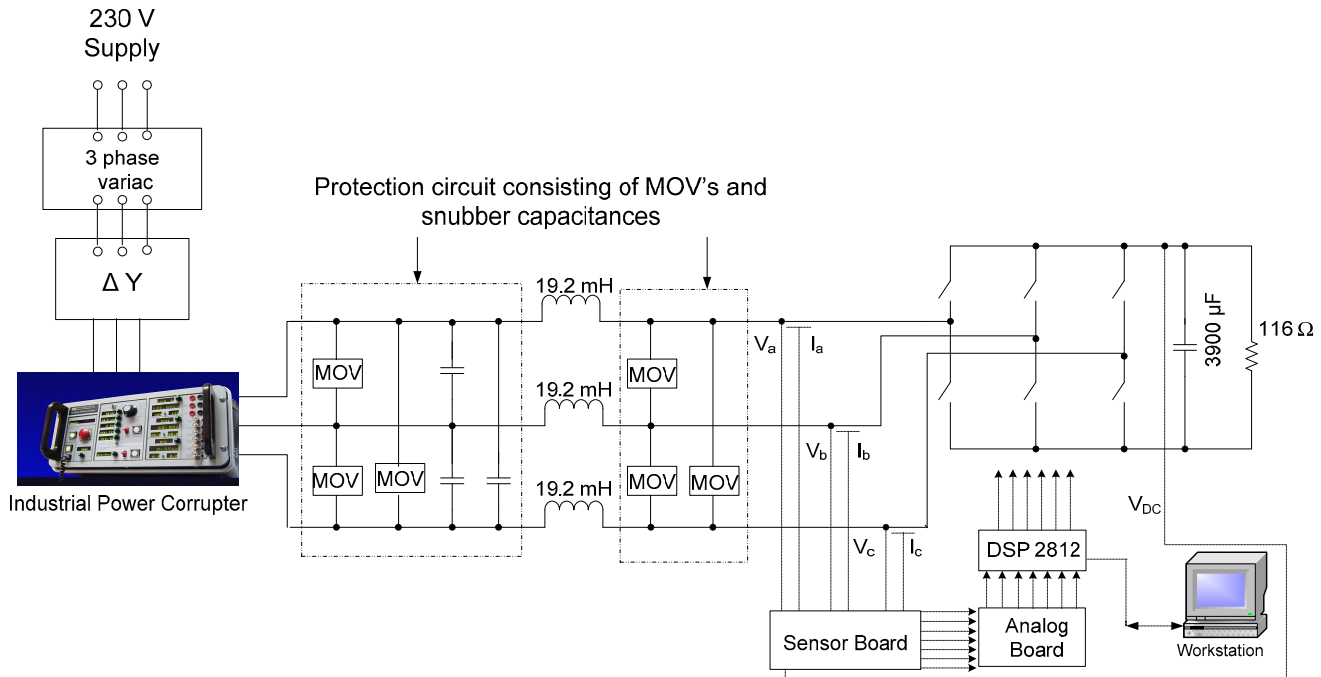


Figure 6. Experimental setup.

[5] J. Eloy-Garcia, S. Arnaltes, J. L. Rodriguez-Amenedo, "Extended direct power control of a three-level neutral point clamped voltage source

inverter with unbalanced voltages," in *Rec. IEEE Power Electronics Specialists Conference*, pp.3396-3400, 2008.

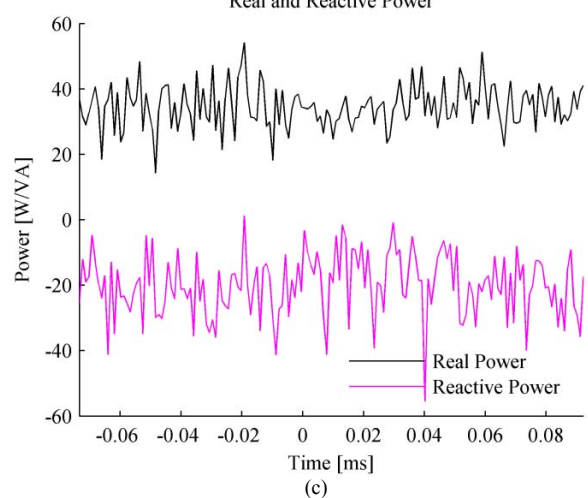
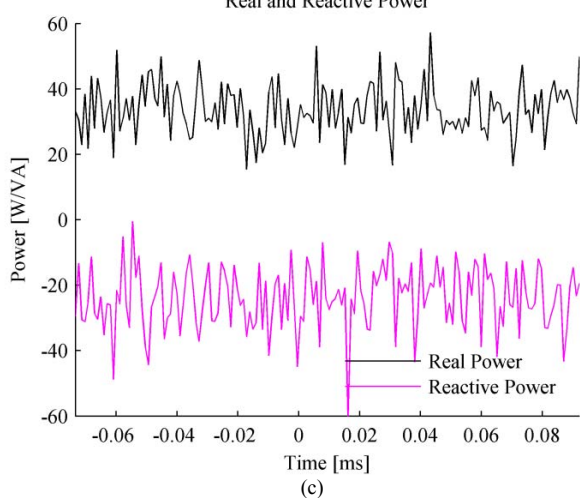
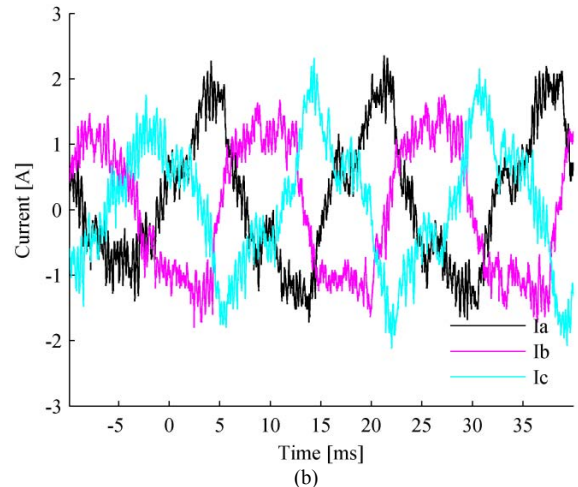
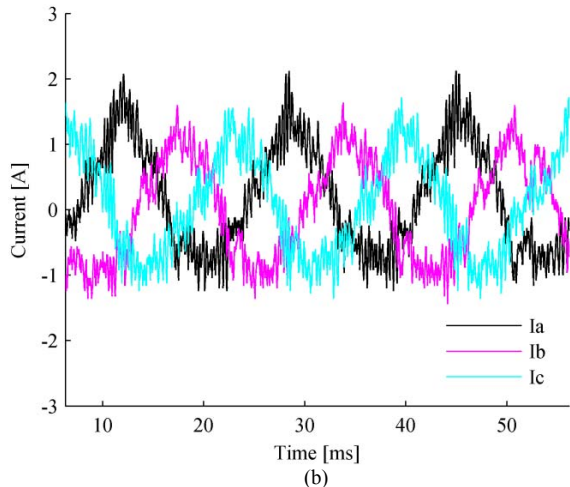
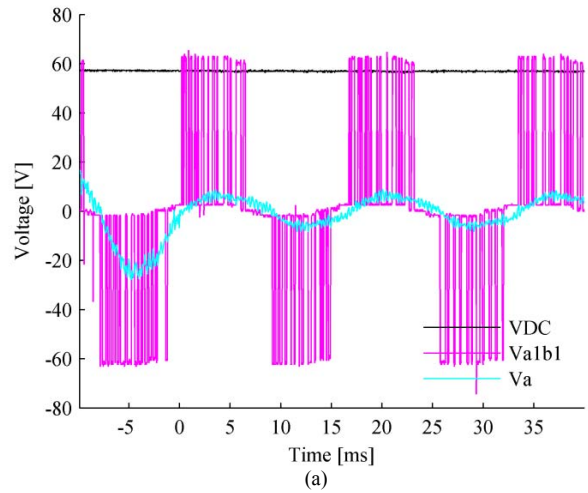
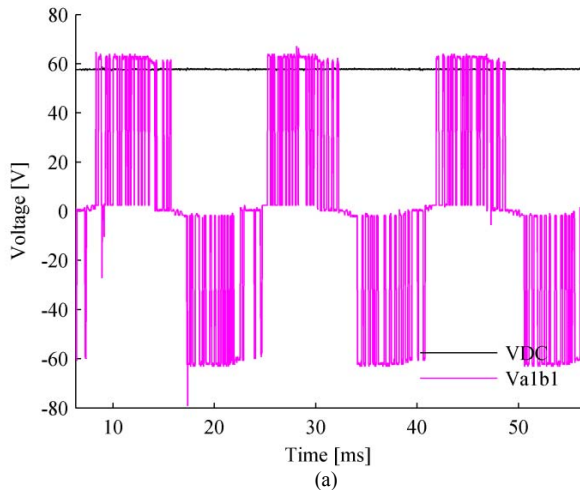


Figure 7. DPC during normal operation. (a) DC bus voltage and switched output voltage, (b) three-phase line currents, (c) real and reactive power.

Figure 8. DPC during a 30% sag on Va (which occurs at time 0 and lasts for 50 ms). (a) DC bus voltage and switched output voltage, (b) three-phase line currents, (c) real and reactive power.